NRC Publications Archive
Archives des publications du CNRC

Production of α2,6-sialylated IgG1 in CHO cells

Raymond, Céline; Robotham, Anna; Spearman, Maureen; Butler, Michael; Kelly, John; Durocher, Yves

NRC Publications Record / Notice d'Archives des publications de CNRC:
https://nrc-publications.canada.ca/eng/view/object/?id=e6369b2f-f442-4fe0-96b1-6e446ebe188f
https://publications-cnrc.canada.ca/fra/voir/objet/?id=e6369b2f-f442-4fe0-96b1-6e446ebe188f

National Research Council Canada   Conseil national de recherches Canada

Canada

mAbs

Production of α2,6-sialylated IgG1 in CHO cells

Céline Raymond[ab], Anna Robotham[c], Maureen Spearman[d], Michael Butler[d], John Kelly[c] &
Yves Durocher[ab]

[a] Human Health Therapeutics Portfolio; National Research Council of Canada; Montreal,
Canada

[b] Department of Biochemistry and Molecular Medicine; Université de Montréal; Montreal,
Canada

[c] Human Health Therapeutics Portfolio; National Research Council of Canada; Ottawa,
Canada

[d] Department of Microbiology; University of Manitoba; Winnipeg, Canada
Accepted author version posted online: 15 Apr 2015.

Click for updates

PLEASE SCROLL DOWN FOR ARTICLE

Production of α2,6-sialylated IgG1 in CHO cells

Céline Raymond[1,2], Anna Robotham[3], Maureen Spearman[4], Michael Butler[4], John Kelly[3], and Yves Durocher[1,2,*]

[1]Human Health Therapeutics Portfolio; National Research Council of Canada; Montreal, Canada; [2]Department of Biochemistry and Molecular Medicine; Université de Montréal; Montreal, Canada; [3]Human Health Therapeutics Portfolio; National Research Council of Canada; Ottawa, Canada; [4]Department of Microbiology; University of Manitoba; Winnipeg, Canada

The presence of α2,6-sialic acids on the Fc N-glycan provides anti-inflammatory properties to the IgGs through a mechanism that remains unclear. Fc-sialylated IgGs are rare in humans as well as in industrial host cell lines such as Chinese hamster ovary (CHO) cells. Facilitated access to well-characterized α2,6-sialylated IgGs would help elucidate the mechanism of this intriguing IgG's effector function. This study presents a method for the efficient Fc glycan α2,6-sialylation of a wild-type and a F243A IgG1 mutant by transient co-expression with the human α2,6-sialyltransferase 1 (ST6) and β1,4-galactosyltransferase 1 (GT) in CHO cells. Overexpression of ST6 alone only had a moderate effect on the glycoprofiles, whereas GT alone greatly enhanced Fc-galactosylation, but not sialylation. Overexpression of both GT and ST6 was necessary to obtain a glycoprofile dominated by α2,6-sialylated glycans in both antibodies. The wild-type was composed of the G2FS(6)1 glycan (38%) with remaining unsialylated glycans, while the mutant glycoprofile was essentially composed of G2FS(6)1 (25%), G2FS(3,6)2 (16%) and G2FS(6,6)2 (37%). The α2,6-linked sialic acids represented over 85% of all sialic acids in both antibodies. We discuss how the limited sialylation level in the wild-type IgG1 expressed alone or with GT results from the glycan interaction with Fc's amino acid residues or from intrinsic galactosyl- and sialyl-transferases substrate specificities.

Introduction

The efficacy of many therapeutic monoclonal antibodies (mAbs) relies on their Fc-dependent effector functions.[1-3] For example, antibody-dependent cell-mediated cytotoxicity (ADCC) or complement-dependent cytotoxicity (CDC) are triggered when the Fc domain interacts with the Fcγ receptors (FcγR) present at the surface of immune cells or the complement molecule C1q, respectively. The Fc domain of immunoglobulin (Ig) G possesses 2 N-glycans, one on each heavy chain (HC) at Asparagine 297, which are necessary for its binding to FcγRs[4-6] or C1q.[7,8]

N-glycosylation is a very common co-translational modification initiated in the endoplasmic reticulum (ER) and completed in the Golgi apparatus. While the antibody progresses in the secretory pathway, the monosaccharide chains are sequentially trimmed and elongated by glycosyltransferases distributed along the ER and Golgi compartments. Glycan modifications happening in the Golgi typically occur when the protein quaternary structure is established. While N-glycans are normally exposed at the surface of the proteins, the Fc N-glycans lie within a pocket formed by the 2 C_H2 domains of the antibody where they interact with internal amino acid residues through hydrogen and CH-π bonds.[9-11] As a consequence of this embedment, the Fc N-glycans are mostly limited to di-antennary complex type with partial galactosylation and low sialylation. The most common glycan on circulating human IgGs is a fucosylated complex structure with one galactose (G1F), followed by fucosylated complex glycans with 0 and 2 galactoses (G0F and G2F) (**Fig. 1**). In addition, 10–20% of IgGs are sialylated (mostly G2FS1).[12-14]

The Fc glycan structure of an IgG impacts its effector functions. For example, core-fucosylation has been shown to decrease Fc binding to FcγRIIIa,[6,15,16] which significantly reduces ADCC.[17,18] In addition, the presence of terminal galactose has been shown to induce conformational changes in the Fc domain,[10] increasing Fc binding to C1q which promotes
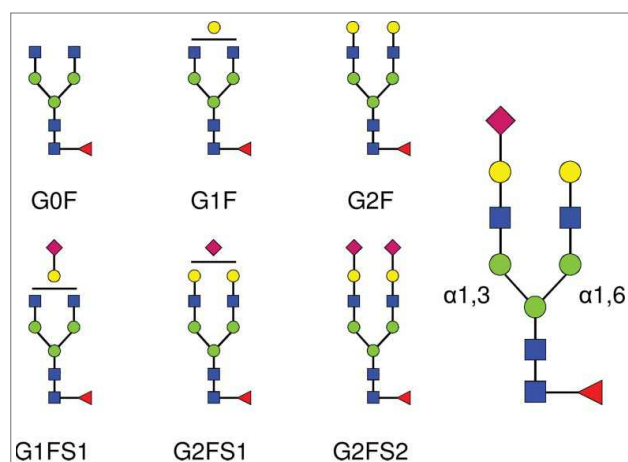
Figure 1. Complex biantennary N-linked glycan structures found in the Fc domain of IgGs. All complex glycans are composed of 4 N-acetylglucosamine residues (GlcNAc, blue squares), and 3 mannose residues (green circles). G0, G1, G2 indicate 0, 1 or 2 galactose residues (yellow circles). F indicates the presence of a core-fucose residue (red triangle). S1 and S2 indicate mono- and di-sialylated glycans (sialic acids are represented as purple diamonds). The sialic acid linkage type is indicated when required in parentheses: G1FS(3)1 and G1FS(6)1 designate G1FS1 carrying either a α2,3- or a α2,6-linked sialic acid, respectively. Similarly, G2FS1 may be G2FS(3)1 or G2FS(6)1. G2FS(3,3)2, G2FS(3,6)2 and G2FS(6,6)2 designate G2FS2 carrying 2 α2,3SA, one α2,3SA and one α2,6SA, or 2 α2,6SA, respectively. α1,3 and α1,6 designate the linkage types of the core mannose residues, and by extension refer to the branches initiated by these residues: the α1,3-arm and the α1,6-arm, respectively.

CDC.[19,20] However, the effect of galactosylation on FcγRIIIa binding or ADCC is unclear.[6,19,20] The impact of the presence of terminal sialic acid residues is also uncertain.[21-30] Indeed, the discrepancies in the methods used for evaluating biological activity, the variability in the type and level of sialylation, as well as the lack of a systematic in-depth glycan characterization, all contribute to the ambiguity of its role in IgG functions. In humans, sialic acids can be attached to the Fc-glycans either on the C3- or the C6-hydroxyl group of the terminal galactose, through the action of α2,3-sialyltransferases (ST3) or the α2,6-sialyltransferase-1 (ST6).[31] Although Fc-sialylation in circulating human IgGs is generally believed to be mainly – if not only – of α2,6 type,[4,32-36] the impact of Fc sialylation on IgG's ADCC was only tested using antibodies bearing exclusively α2,3-linked sialic acids (α2,3SA).[22] Contradictory results were also reported on sialylated Fcs' ability to bind FcγRIIIa, but using dissimilar IgG preparations and affinity measurement protocols.[21,28] In other studies assessing the anti-inflammatory properties of α2,6-sialylated IgGs,[21,24,26,30] blood-derived or recombinant antibodies were enriched by affinity chromatography using *Sambucus Nigra agglutinin*-resins that were shown to catch mainly IgGs bearing Fab-sialylated glycans to the detriment of Fc-sialylated species.[24,32,37] While the specific involvement of Fc's α2,6-sialylation in anti-inflammatory activity was shown by Anthony et al. in their model,[35] which receptor the sialylated Fcs are targeting remains controversial.[23,27,30] A method for the rapid production of IgGs with physiological and well-characterized α2,6-sialylated

Fc would thus greatly help to better characterize their mechanism of action.

Approaches developed to enhance sialylation of IgG's Fc-glycans fall into 3 major categories: (1) in vitro enzymatic glycan remodeling of purified antibodies, (2) engineering of Fc amino-acid sequence, or (3) cell engineering through the over-expression of glycosyltransferases. The in vitro enzymatic addition of galactose and sialic acid residues on purified mAbs was shown to be effective, but requires several 24 hour-cycles of reaction, substantial amounts of costly recombinant enzymes and substrates, and an additional purification step.[35,38,39] Single amino acid mutations in the Fc, such as the replacement of the phenylalanine 243 by an alanine that disrupts the glycan-CH2 domain interaction,[33,40] were shown to allow enhanced galactosylation and sialylation, reinforcing the hypothesis that glycan embedment and interaction with the Fc structure may limit its access to some glycosyltransferases. However, amino acid substitutions lying far away from the glycan were also shown to affect glycosylation and receptor binding.[41,42] The very high number of potent mutations and the possibility that the mutations themselves rather than the resulting altered glycan structure may affect antibody function render the understanding of Fc glycan structure/function a complex task.[28]

Most cell engineering efforts directed toward altering glycosylation have focused on the manipulation of Chinese hamster ovary (CHO) cell lines because they are widely used for the manufacturing of therapeutic mAbs.[43] Their glycosylation machinery is very similar to that of humans, but they lack a functional ST6, limiting their sialylation capability to the addition of α2,3SA residues.[44] Moreover, IgGs produced in CHO cells appear to be severely hypogalactosylated.[40] The stable expression of human ST3 and β1,4-galactosyltransferase 1 (GT) together with a tumor necrosis factor receptor-IgG1 (TNFR-IgG1) fusion protein, allowed increased sialylation,[45] but the highly-branched and highly-sialylated TNFR N-glycans did not allow clear assessment of Fc sialylation. In another study, the untranslated ST6 gene present in the CHO genome was cloned and reinserted, providing a functional ST6, which led to a good enhancement of IgG's sialylation, but the growth and viability of the CHO cells expressing ST6 were significantly affected.[46] Finally, it was shown that the co-expression of a rat ST6 with a mutant F243A IgG3 did not increase the overall Fc sialylation level, but rather resulted in a α2,6:α2,3 sialic acid ratio of 0.9:1.[33] Interestingly, this work also showed that the α2,3-sialylated F243A mutant had no affinity for FcγRI, FcγRII, and C1q, while the same mutant containing 50% of α2,6SA residues showed affinity for these receptors similar to that of the wild-type IgG3, highlighting the importance of properly determining the type of sialic acid linkage.

In this study, we developed a method for the fast production of α2,6-sialylated IgG1 by transient co-expression of human GT, ST6 and IgG1 in CHO cells. The mAbs used as models were the humanized trastuzumab (TZM) IgG1 antibody possessing a human Fc, and its F243A mutated version. The effect of co-expressing GT, ST6, or both on Fc glycans was analyzed by liquid chromatography coupled to electrospray ionization mass

spectrometry (LC-ESI-MS). The nature of the sialic acid linkage was assessed by sequential sialidase digestions followed by capillary zone electrophoresis isoelectric focusing (cIEF), and hydrophilic interaction liquid chromatography (HILIC). We showed that significant levels of physiologically relevant monosialylated glycan, as those found on circulating human IgGs, were found on TZM Fc following the co-expression of GT and ST6. Comparison of the wild-type and F243A mutant glycoprofiles suggests that glycan interaction with F243 hampers the action of CHO and human GT as well as ST6. Also, our data indicate that the overexpression of human GT and ST6 in CHO cells significantly favors α2,6-sialylation over α2,3-sialylation.

Results

Production of sialylated antibodies

TZM was expressed by co-transfection of 2 plasmids, one coding for the HC and the other coding for the light chain (LC). A HC:LC ratio of 2:3 (w:w) was used to ensure optimal expression of the mAb in CHO-3E7 cells as determined in a previous work.[47] The human membrane-associated β-1,4-galactoyltransferase 1 (GT) and β-galactoside α-2,6-sialyltransferase 1 (ST6) were co-expressed with the mAbs to enhance galactosylation or α2,6-sialylation of the Fc. The quantity of GT-encoding plasmid necessary to achieve maximal galactosylation of the Fc was first assessed. Between 0.5% to 10% (w:w) of GT plasmid was

Figure 2. Lectin-blot analyses of TZM from culture supernatants. Various amounts of glycosyltransferases and harvest time were tested for optimal galactosylation and sialylation of the Fc. The lectin-blots show the mAbs' heavy chain (reducing gels). Ponceau red staining was used to control the protein load. Panel (**A**) Co-expression of TZM and GT. The DNA mix was composed of 0% to 10% in weight of GT encoding plasmid, the rest being a 6:4 mixture of plasmids coding for TZM light and heavy chains. ECL was used to detect terminal galactosylation. Panel (**B**) Co-expression of TZM, GT and ST6. The DNA mix was composed of 2% of GT plasmid with 0% to 20% of ST6 coding plasmid, the rest being a 6:4 mixture of plasmids coding for TZM light and heavy chains. SNA was used to detect terminal α2,6-sialylation. Panel (**C**) HC α2,6-sialylation level from day 2 to day 9 post-transfection.

incorporated into the DNA mix, for a final DNA concentration of 1 μg per mL of culture to be transfected. The extent of Fc glycan galactosylation was determined by lectin-blot using the *Erythrina cristagalli* lectin (ECL) that specifically detects terminal galactoses. The blot showed that 2% of GT encoding plasmid was sufficient to allow maximal galactosylation of the HC (**Fig. 2A**). The assay was repeated with a 98:2 (w:w) TZM:GT plasmid ratio and various amounts of the ST6 encoding plasmid. The *Sambucus nigra* lectin (SNA) was used to evaluate α2,6-sialylation. As previously reported, 20% of ST6 plasmid in the transfection mix was optimal for HC sialylation (**Fig. 2B**).[47] The DNA mix composition selected was thus 2% of GT plasmid and 20% of ST6 plasmid (**Fig. 2A–B**). Next, we assessed the optimal harvest time that produced the highest α2,6-sialylation level of the Fc. HC α2,6-sialylation was monitored by SNA-blot from 2 d post-transfection (dpt) until day 9 post-transfection where cell viability dropped to ~40%. The cultures were shifted from 37°C to 32°C at 1 dpt to delay cell death and increase production yields.[48] The harvest time was set at 4 dpt to get an optimal Fc sialylation while allowing for acceptable TZM yields of ~15–20 mg/L after protein-A purification (**Fig. 2C**).

Antibody characterization

These optimal conditions were scaled up to 500 mL cultures to produce milligrams of TZM expressed alone or co-expressed with GT, ST6 or both (designated GT, ST6 or GTST6, respectively). The TZM containing the F243A substitution (TZMm) was also produced under the same conditions. All antibodies were obtained at yields of ~15–20 mg/L. Following protein-A purification, the sialylation levels were first evaluated by cIEF and lectin-blotting. **Figure 3A** shows that TZM IEF profile was defined by a main charge variant flanked by very low amounts of 2 basic variants and 2 acidic variants. A non-glycosylated version of TZM, the N297Q mutant, exhibited the same profile, showing that the basic and acidic variants were not due to Fc glycan. In contrast, TZMm exhibited high levels of acidic variants. Its desialylation by an α2,3SA-specific sialidase (sialidase S) resulted in the complete loss of these acidic variants, confirming that appearance of these acidic variants on cIEF is the consequence of sialylation. Interestingly, TZMGT and TZMST6 showed the same cIEF profile as TZM, whereas TZMGTST6 and the 4 TZMm samples (+/− GT and/or ST6) had patterns differing in number, pI and intensity of acidic variants (**Fig. 3B** panel 1). SNA-blotting confirmed the presence of α2,6SA in TZMGTST6, TZMmST6 and TZMmGTST6, but no signal was detected in TZMST6, supporting IEF results (**Fig. 3B** panel 2). *Maackia amurensis* lectin II (MALII)-blotting was then used to detect endogenous CHO α2,3-sialylation, which was only detectable in the 4 TZMm samples. The strongest signal was obtained when TZMm was expressed alone (**Fig. 3B** panel 3), declined when GT or ST6 were co-expressed, and became almost undetectable in the presence of both GT and ST6. Finally, the presence of terminal galactose residues was assessed using the *Erythrina cristagalli* lectin (**Fig. 3B** panel 4). No or only barely detectable ECL signal was detected when TZM or TZMm were expressed alone or co-expressed with ST6. However, a strong
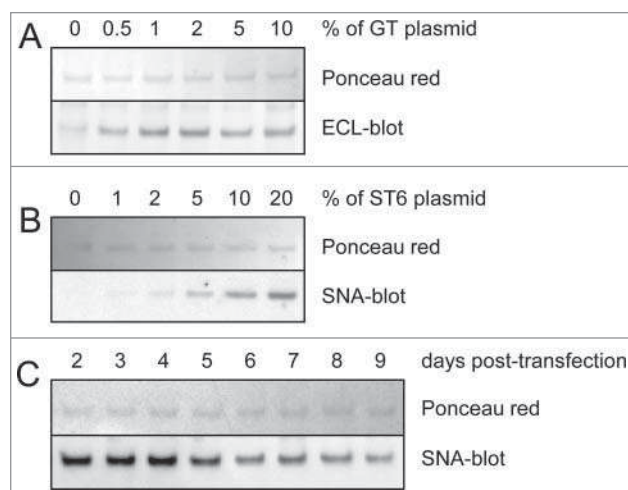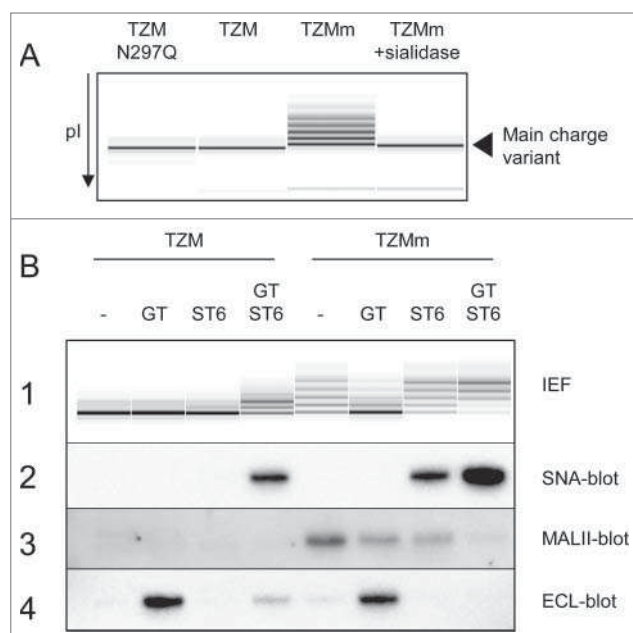
Figure 3. Capillary IEF (cIEF) electropherograms of TZM constructs. Panel (**A**) The cIEF profile of TZM is composed of a main charge variant and traces of acidic and basic variants. These traces are not the result of glycosylation since the non-glycosylated mutant TZM N297Q has an identical profile. In contrast, the acidic variants of TZMm are the result of sialylation. Panel (**B1**) cIEF profiles of purified TZM and TZMm expressed alone or in the presence of GT, ST6, or both. Panel (**B2–4**) Lectin-blots showing the α2,6-sialylation, α2,3-sialylation and terminal galactosylation levels of TZM heavy chain as revealed by SNA, MALII and ECL, respectively.

Glycan analyses by mass spectrometry

To confirm these observations and describe further the effect of the F243A mutation and co-expression of glycosyltransferases on TZM glycoprofiles, the antibodies were submitted to LC-ESI-MS analysis. They were first digested by the immunoglobulin-degrading enzyme from *Streptococcus pyogenes* (IdeS), which cleaves the antibody into a F(ab')2 fragment and 2 Fc/2 (C_H2-C_H3) glycosylated polypeptides. The molecular weight profiles obtained for the Fc/2 glycopeptides by LC-ESI-MS are shown in **Figure 4** and their relative intensities are presented in **Table 1**. For each mAb, the relative peak intensities were used to calculate the relative number of branches terminated by a given monosaccharide residue among the complex glycans (**Table 2**). Non-glycosylated Fc/2 peptides were not detected in any of the 8 conditions, confirming the full occupancy of the N297 glycosylation site in all antibodies.

TZM showed the classical glycoprofile of CHO-produced IgG1, i.e., a large majority of fucosylated non-galactosylated glycans (G0F, 54.4 ± 1.9%), followed by monogalactosylated glycans (G1F, 31.4 ± 2.1%) and small amounts of fully galactosylated glycans (G2F, 5.1 ± 0.1%) (**Fig. 4A**). As suggested by the cIEF and lectin-blot results, ST6 expression had negligible effect on TZM glycan (**Fig. 4B**); only small amounts of the mono-sialylated species G1FS1 and G2FS1 (5.8 ± 0.7% and 2.7 ± 0.7%, respectively) were obtained. To estimate the sialylation efficiency independently of the composition of the glycan pool, we expressed the sialylation level in relative number of antennae carrying a sialic acid among the complex glycan branches, i.e., excluding high-mannose and hybrid glycan branches (see the Materials and Methods Section for the formula employed). We found that only 4.8 ± 0.1% of the complex antennae were terminated by a sialic acid in TZMST6 (**Table 2**). However, expression of GT dramatically modified TZM glycoprofile as seen on the m/z profile (**Fig. 4C**); G2F became the predominant glycan (44.8 ± 2.1%), and the percentage of complex antennae terminated by a galactose increased from 22.7 ± 0.4% in TZM to 66.4 ± 1.2% in TZMGT (**Table 2**). Although it could not be seen by cIEF and

signal appeared when both mAbs were co-expressed with GT, indicating efficient galactosylation. The ECL signal was significantly reduced when TZM was co-expressed with GT and ST6 while it completely disappeared in the case of TZMmGTST6, indicating efficient sialylation by ST6.

Table 1. Fc glycan composition of the wild-type TZM and F243A mutant expressed alone or co-expressed with GT, ST6 or both. The values are averages of relative peak heights in the molecular weight profiles obtained by LC-ESI-MS of Fc/2 glycopeptides of 2 independent batches. The category "other tri-antennae" contains glycans having a third complex branch being partially sialylated or galactosylated (e.g. G3FS2). High-mannose glycans comprise M5, M6, M7, M8 and M9 The category "truncated core" contains the hybrid glycans Galβ1–4GlcNAcβ1–2Manα1–3/6(Manα1–6/3)Manβ1–4GlcNAcβ1–4(Fucα1–6)GlcNAc (abbreviated here as G1F−GlcNAc), GlcNAcβ1–2Manα1–3/6(Manα1–6/3)Manβ1–4GlcNAcβ1–4(Fucα1–6)GlcNAc (G0F−GlcNAc), and GlcNAcβ1–2Manα1–3/6Manβ1–4GlcNAcβ1–4(Fucα1–6)GlcNAc, as well as the Fucα1–6GlcNAc fragment (GlcNAcF), which was found in one of the 2 batches only, but represented 2 to 6% in the wild-type mab, and up to 10–15% in the mutant

	TZM (%)	TZMGT (%)	TZMST6 (%)	TZMGTST6 (%)	TZMm (%)	TZMmGT (%)	TZMmST6 (%)	TZMmGTST6 (%)
G0F	54.4 ± 1.9	15.0 ± 1.4	49.6 ± 4.6	12.3 ± 1.4	8.3 ± 2.3	0.0	9.9 ± 0.2	0.6 ± 0.8
G1F	31.4 ± 2.1	23.5 ± 4.2	26.3 ± 1.5	19.5 ± 1.4	19.4 ± 0.4	3.5 ± 0.3	14.9 ± 2.9	1.4 ± 0.3
G2F	5.1 ± 0.1	44.8 ± 2.1	3.5 ± 0.1	20.9 ± 2.9	11.4 ± 1.1	41.0 ± 0.5	2.3 ± 0.1	2.9 ± 0.4
G3F	0.0	0.0	0.0	0.0	0.0	2.2 ± 0.0	0.0	0.0
G1FS1	0.9 ± 1.3	0.6 ± 0.8	5.8 ± 0.7	2.4 ± 0.3	14.3 ± 4.3	2.2 ± 0.4	19.8 ± 3.3	2.8 ± 0.6
G2FS1	0.0	3.5 ± 1.2	2.7 ± 0.7	32.0 ± 1.0	16.7 ± 0.6	19.9 ± 5.6	13.4 ± 1.3	29.1 ± 4.0
G2FS2	0.0	0.5 ± 0.7	0.0	6.6 ± 0.8	19.6 ± 0.2	17.0 ± 6.3	28.6 ± 1.2	50.4 ± 4.4
G3FS3	0.0	0.0	0.0	0.0	4.3 ± 0.8	1.3 ± 1.8	5.0 ± 0.7	2.6 ± 1.4
Other tri-antennae	0.0	0.0	0.0	0.0	0.0	0.0	1.1 ± 0.1	2.6 ± 1.0
High-mannose	5.3 ± 1.7	6.8 ± 4.2	4.8 ± 1.3	4.7 ± 2.7	0.6 ± 0.8	4.4 ± 2.7	0.0	2.0 ± 2.9
Truncated core	2.9 ± 1.0	5.3 ± 4.7	6.9 ± 3.6	1.6 ± 2.2	5.4 ± 7.6	8.6 ± 12.2	5.0 ± 7.1	5.7 ± 8.0

Table 2 Incidence of terminal GlcNAc, galactose and sialic acid residues in the composition of the antennae of the complex glycans (i.e., the glycans presented in **Table 1**, except for the high-mannose and truncated-core categories) (rows 1, 2 and 3, respectively). A complex antenna is defined here by the sequence GlcNAcβ1–2Manα1–3/6Manβ1–4GlcNAcβ1–4GlcNAc. The incidence of Gal residues (either terminal of SA-capped), as well as the proportion of Gal residues capped with a SA were also calculated (rows 4 and 5, respectively). These results are based on the LC-ESI-MS analyses

	TZM	TZMGT	TZMST6	TZMGTST6	TZMm	TZMmGT	TZMmST6	TZMmGTST6
Arms terminated by a GlcNAc (%)	76.8 ± 0.3	30.7 ± 0.4	74.7 ± 2.2	24.9 ± 1.9	26.1 ± 2.4	3.2 ± 0.2	28.0 ± 1.3	2.7 ± 1.0
Arms terminated by a Gal (%)	22.7 ± 0.4	66.4 ± 1.2	20.5 ± 2.1	49.7 ± 1.7	30.7 ± 1.7	63.7 ± 7.5	17.3 ± 0.2	21.1 ± 1.0
Arms terminated by a SA (%)	0.5 ± 0.7	2.9 ± 0.8	4.8 ± 0.1	25.4 ± 0.2	43.2 ± 0.7	33.1 ± 7.7	54.7 ± 1.5	76.2 ± 0.1
Arms carrying a Gal (%)	23.2 ± 0.3	69.3 ± 0.4	25.3 ± 2.2	75.1 ± 1.9	73.9 ± 2.4	96.8 ± 0.2	72.0 ± 1.3	97.3 ± 1.0
Gal capped by a SA (%)	2.2 ± 3.2	4.2 ± 1.2	19.1 ± 1.1	33.9 ± 0.6	58.5 ± 1.0	34.2 ± 7.9	76.0 ± 0.7	78.4 ± 0.8

lectin-blot analyses, the presence of terminal sialic acid was detected at low level (4.6 ± 0.6% of glycans), despite the abundance of terminal galactose residues available for the CHO endogenous ST3 enzyme. Upon co-expression of both GT and ST6, the amount of G2F significantly decreased compared to TZMGT (20.9 ± 2.9% vs 44.8 ± 2.1%) while G2FS1 increased to 32.0 ± 1.0%, becoming the major glycan found in TZMGTST6 sample (**Fig. 4D**). However, only a little amount of G2FS2 was detected (6.6 ± 0.8%). In contrast with the TZM produced in the other 3 conditions, where less than 5% of the complex glycan branches were sialylated, up to 25.4 ± 0.2% of the complex glycan branches were terminated by a sialic acid in TZMGTST6 (**Table 2**). These results confirmed that both GT and ST6 were necessary to raise sialylation of the wild-type TZM to high levels as previously suggested by the cIEF analysis.

Impact of the F243A mutation

The F243A mutation resulted in a sharp increase in the glycan heterogeneity compared to the wild-type TZM (**Fig. 4E**). This was a direct consequence of the appearance of the sialylated glycans G1FS1, G2FS1 and G2FS2, representing ~14%, 17% and 20%, respectively, of the glycan species. This increased sialylation was enabled by a high level of galactosylation compared to the wild-type antibody; the proportion of complex glycan arms carrying a galactose residue, either terminal or capped with a SA, increased from 23.2 ± 0.3% in TZM up to 73.9 ± 2.4% in TZMm (**Table 2**). Similarly to TZMST6, the co-expression of the F243A mutant with ST6 resulted in a moderate 11.5% increase in the relative number of complex arms terminated by a SA (**Fig. 4F, Table 2**),

while its co-expression with human GT resulted in >95% of the complex glycan branches carrying a galactose (**Table 2**). Interestingly, and as observed with TZMGT, G2F was the dominant species (41.0 ± 0.5%) in TZMmGT
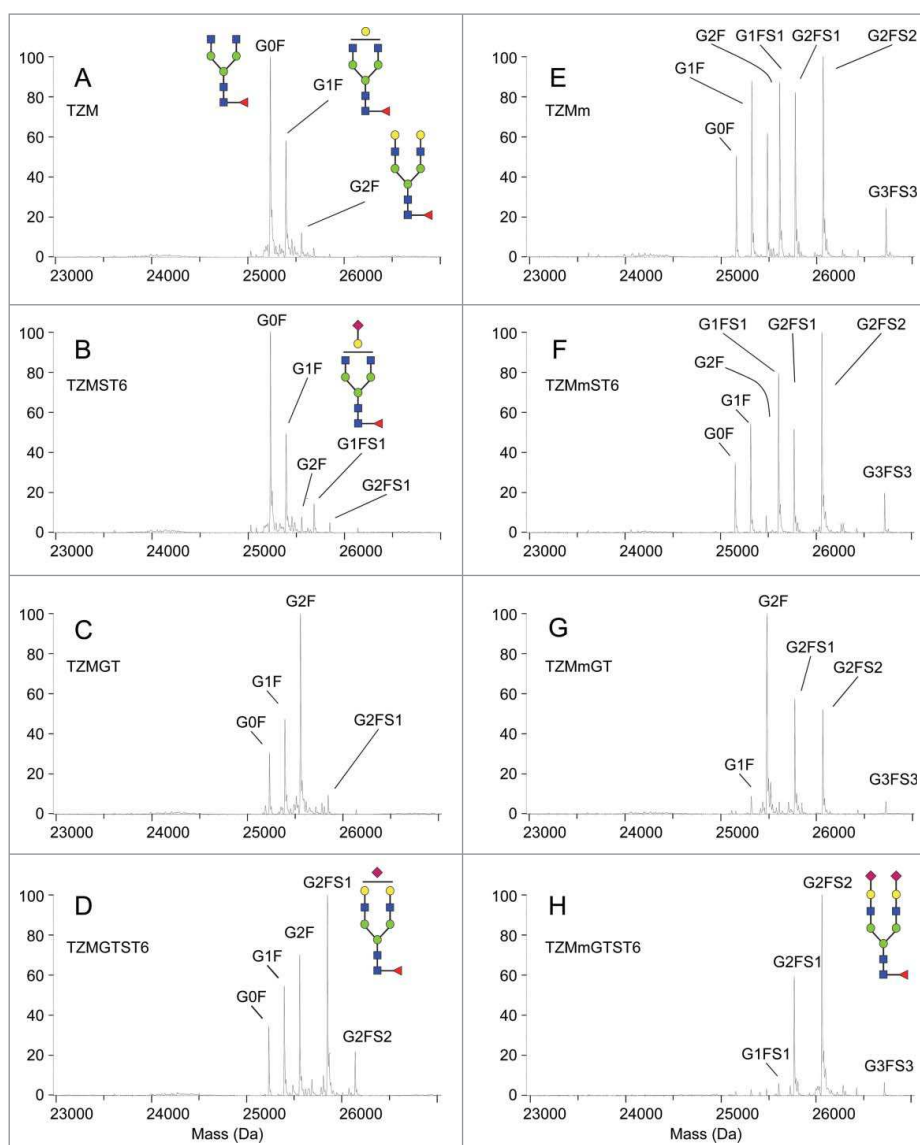

Figure 4. Fc/2 molecular weight profiles obtained by LC-ESI-MS analysis. The analysis was performed on 2 independent batches. Secondary peaks were detected at +16 Da for all glycopeptides and were considered to be caused by oxidation.

(**Fig. 4G**). However, this increased galactosylation did not lead to a higher sialylation; the sialylation level was even lower in TZMmGT than in TZMm (40% and 55% of sialylated glycans, respectively). Finally, the TZMmGTST6 glycans were mostly sialylated (**Fig. 4H** and **Table 1**); G2FS2 and G2FS1 were the predominant glycans (50.4 ± 4.4%

and 29.1 ± 4.0%, respectively), meaning that over 75% of the complex glycan branches were terminated by a sialic acid (**Table 2**). Moreover, 78% of the galactoses were sialylated compared to only 34% in TZMGTST6 (**Table 2**), suggesting that the F243A mutation greatly improves ST6-mediated sialylation.

Figure 5. Effect of α2,3SA-specific sialidase S treatment on TZM samples. Panel (**A**) cIEF profiles TZM and TZMm; panels (**B–D**) HILIC profiles of TZMGTST6, TZMmST6 and TZMmGTST6. HILIC was performed on PNGaseF-released glycans from 2 independent batches (u.g. stands for unidentified glycan). Non-specific digestion was suspected in TZMmST6 (Panel C). Unexpected high absorbance is indicated by (*), and unexpected low absorbance by (**). GlcNAcF refers to the Fucα1–6GlcNAc fragment.

Determination of sialic acid linkage type

Considering the extremely low level of α2,3-sialylation in TZMGT, we hypothesized that the sialic acids in TZMGTST6 glycans were mostly – if not only – of the α2,6 type, whereas in the mutants TZMmST6 and TZMmGTST6, the sialylated glycans could contain a mixture of α2,3- and α2,6-linked SA. The SA linkage types in the glycans were assessed by cIEF and HILIC analysis after digestion with the α2,3SA-specific sialidase S from *Streptococcus pneumoniae* or the non-specific sialidase A from *Arthrobacter ureafaciens*.

TZMGTST6

Specific α2,3SA digestion with Sialidase S had no effect on the cIEF profile of TZMGTST6 (**Fig. 5A**), in agreement with the absence of signal on the MALII-blot (see **Fig. 3B** panel 3). This was also confirmed by HILIC analysis of sialidase S treatment of PNGaseF released Fc-glycans (**Fig. 5B**). The G0F, G1F, G2F and G2FS1 glycans were detected in increasing amounts, in accordance with LC-ESI-MS analyses. The correlation between the glycans relative abundances as detected by MS and HILIC analyses of TZMGTST6 was very good (Pearson correlation coefficient P = 0.95). G2FS1 mainly appeared (95%) as an α2,6-sialylated isomer G2FS(6)1 (37.6 ± 4.0%) eluting at a retention time (RT) of 41.2 min (**Table 3**). It is noteworthy that G2FS (6)1 eluted on some occasions at a higher RT corresponding to the G2FS (3,3)2 glycan, but each time the peak was not sensitive to sialidase S digestion (data not shown). The peak at RT = 42.4 min was attributed to the disialylated glycan G2FS(3,6)2 (4.1 ± 1.1%), although a small peak remaining after sialidase S treatment suggested the presence of a co-eluting compound (**Fig. 5B, C & D**). G2FS(6,6)2 was also

Table 3. Fc glycan composition of the wild-type TZM co-expressed with GT and ST6, and the F243A mutant (TZMm) co-expressed with ST6 alone or GT and ST6. The values are averages of the peak areas obtained in the HILIC chromatograms of PNGaseF-released glycans from 2 independent batches. Although significant amounts of G3FS3 were detected by LC-ESI-MS, no peak could be attributed with certitude to this glycan in HILIC chromatograms, because of their numerous potential isoforms. The peaks with a GU value $\geq$ 9.60, affected by sialidases, were thus grouped in the category "presumed triantennae," and the incidence of $\alpha2,3$ and $\alpha2,6$SA was calculated on the glycans G1FS1, G2FS1 and G2FS2 only

	Retention time	GU value	TZMGTST6 (%)	TZMmST6 (%)	TZMmGTST6 (%)
GlcNAcF	31.3	5.40	0.4 $\pm$ 0.1	0.6 $\pm$ 0.1	0.1 $\pm$ 0.2
G0F	33.2	5.84	9.5 $\pm$ 1.6	8.6 $\pm$ 0.9	1.1 $\pm$ 0.2
G1	34.4	6.15	1.1 $\pm$ 0.1	1.0 $\pm$ 0.0	1.0 $\pm$ 0.6
G1F isomer a	36.0	6.60	13.3 $\pm$ 3.8	12.0 $\pm$ 1.6	2.1 $\pm$ 0.3
G1F isomer b	36.3	6.70	2.0 $\pm$ 0.6	1.2 $\pm$ 0.0	0.0
G2F	38.9	7.48	20.5 $\pm$ 1.9	11.2 $\pm$ 0.7	2.8 $\pm$ 0.5
G1FS(3)1	37.4	7.04	1.0 $\pm$ 0.2	9.4 $\pm$ 2.6	1.9 $\pm$ 0.7
G1FS(6)1	39.3	7.60	1.4 $\pm$ 0.2	2.6 $\pm$ 0.2	0.8 $\pm$ 0.1
G2FS(3)1	40.2	7.94	1.8 $\pm$ 0.9	5.3 $\pm$ 0.6	2.8 $\pm$ 0.1
G2FS(6)1	41.3	8.38	37.6 $\pm$ 4.0	12.9 $\pm$ 0.4	24.6 $\pm$ 3.5
G2FS(3,3)2	41.4	8.42	0.0 $\pm$ 0.0	0.0 $\pm$ 0.0	0.0 $\pm$ 0.0
G2FS(3,6)2	42.6	8.80	4.1 $\pm$ 1.1	18.8 $\pm$ 0.9	15.8 $\pm$ 2.0
G2FS(6,6)2	43.6	9.20	3.0 $\pm$ 0.3	11.7 $\pm$ 3.5	37.0 $\pm$ 5.8
Presumed tri-antennae	$\geq$ 44.4	$\geq$ 9.60	0.2 $\pm$ 0.2	3.1 $\pm$ 0.1	2.9 $\pm$ 1.0
Unidentified glycans >2%	38.4 and 40.4	7.30 and 8.04	3.1 $\pm$ 2.8	0.0	4.4 $\pm$ 2.7
total % $\alpha2,6$SA:$\alpha2,3$SA			88:12	63:37	85:15

detected at a low level. It was found that 88% of the sialic acids in TZMGTST6 glycans were of $\alpha2,6$ type (**Table 3** and **Fig. 6**).

TZMmST6

The $\alpha2,3$SA-specific desialylation of TZMmST6 resulted in a drastic decrease in the abundance of the most acidic bands of the cIEF profile (**Fig. 5A**), demonstrating the presence of $\alpha2,3$SA, as supported by MALII-blotting (**Fig. 3B**, panel 3). However, the HILIC profile obtained for TZMmST6 did not fully agreed with the LC-ESI-MS data (Pearson correlation coefficient P = 0.77) (compare **Fig. 5C** with **Fig. 4F**). There were 2 main discrepancies with the LC-ESI-MS profile; first, the glycan G2F (RT = 38.7 min) appeared more abundant in HILIC than in MS (HILIC: 12%; MS: 2%), and second, the G1FS1 glycans (2 isomers at RT = 37.4 and 39.1 min) were less abundant in HILIC than in MS (HILIC: 10%; MS: 17%) (**Figs. 4F and 5C**, **Tables 1 and 3**). Nevertheless, the presence of the $\alpha2,3$-sialylated glycans G1FS(3)1, G2FS(3)1 and G2FS(3,6)2, eluting at 37.4 min, 39.9 min and 42.3 min, respectively, was confirmed by sialidase S digestion (**Fig. 5C**). The $\alpha2,6$-sialylated isomers G1FS(6)1 (RT = 39.1 min), G2FS(6)1 (RT = 41.2 min) and G2FS(6,6)2 (RT = 43.4 min), were also detected, although the peaks appeared altered by the sialidase S treatment (the increased peak intensities of G0F and G1F suggests some non-specific digestion). It was found that G1FS(3)1 was the predominant G1FS1 isoform while G2FS(6)1 was the predominant G2FS1 isoform (**Table 3**). The G2FS2 glycans were a mixture of G2FS(3,6)2 (18.8 $\pm$ 0.9%) and G2FS(6,6)2 (11.7 $\pm$ 3.5%) isoforms. Interestingly the G2FS(3,3)2 isoform was not detected (**Table 3**), suggesting that ST6 is faster than ST3 to sialylate G2FS(3)1. Overall, the predominant SA linkage in TZMmST6 was of the $\alpha2,6$ type (63%), although its predominance over the $\alpha2,3$-

linkage type was less pronounced than in TZMGTST6 (**Table 3** or **Fig. 6**).

TZMmGTST6

The sialidase S treatment resulted in a decreased intensity of the most acidic bands on the cIEF profile (**Fig. 5A**), suggesting the presence of $\alpha2,3$SA in TZMmGTST6 as predicted by the
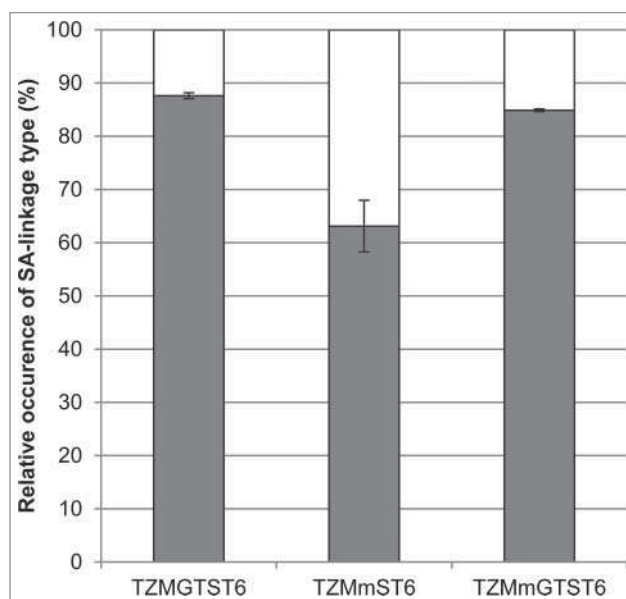

Figure 6. The relative abundances of the sialylated biantennary complex glycans (G1FS1, G2FS1 and G2FS2). The HILIC results were used to calculate the proportion of $\alpha2,3$- and $\alpha2,6$-linked sialic acids found in TZMGTST6, TZMmST6 and TZMmGTST6. White:% $\alpha2,3$SA. Gray:% $\alpha2,6$SA.

MALII-blot (**Fig. 3B**, panel 3). The relative abundances of TZMmGTST6 glycans as determined by HILIC were in very good agreement with those of the corresponding Fc/2 glycopeptides detected by LC-ESI-MS (Pearson correlation coefficient P = 0.99). The chromatogram showed that G2FS(6,6)2 was the major glycan (**Fig. 5D**), (37 ± 5.8%), followed by G2FS(6)1 (24.6 ± 3.5%) (**Table 3**). The G2FS2 isoform G2FS(3,6)2 was the third glycan in abundance (15.8 ± 2.0%) (**Fig. 5D**, **Table 2**), whereas G2FS(3,3)2 was again not found. The predominance of α2,6SA was similar to that found in TZMGTST6 as they represented 85% of all sialic acids present in the G1FS1, G2FS1 and G2FS2 glycans (**Table 3** or **Fig. 6**).

Discussion

The precise impact of Fc-sialylation on CDC and ADCC, and the mechanism by which it has been proposed to confer anti-inflammatory properties to antibodies, have not been fully elucidated. The variety of sialylated glycans (linkage type, branch occupancy) and the low abundance of Fc-sialylated glycans in circulating antibodies or in CHO-produced recombinant mAbs have made difficult the generation of consistent data on their functions. In this study, we present a method for the fast production of highly sialylated mAbs in CHO cells with a well-characterized glycoprofile to enable better assessment of the biological function of Fc-sialylation. Milligram amounts of highly galactosylated IgG1 or G2FS(6)1 enriched IgG1 could be obtained within 2 weeks.

Our data indicated that the co-transfection of both GT and ST6 was required to obtain a wild-type IgG1 with a glycoprofile dominated by monosialylated G2FS1 glycans, as found in circulating human antibodies. Indeed, the expression of ST6 alone resulted in very poor sialylation improvement. Although terminal galactose residues were available in the G1F glycans, they were not efficiently used as substrates by ST6. This could be explained by the selectivity of the human ST6 for the α1,3-branch of the glycan (**Fig. 1**), while the galactose residue present on the main G1F isomer was found on the opposite arm.[39] More surprising, while TZM co-expression with GT was expected to improve terminal sialylation by providing galactose residues for the endogenous ST3, G2F was the major glycan, while only traces of G2FS1 could be detected. Thus, the concomitant expression of ST6 with GT was necessary not only to introduce α2,6-linked SA in the CHO cell, but also to allow the sialylation of the additional galactoses provided by GT. By co-expressing GT and ST6, we obtained >40% of sialylated glycans in the wild-type TZM, with >75% of them being G2FS(6)1. About 25% of the complex branches were terminated by a sialic acid, and 88% of the sialic acids were of the α2,6 type. Onitsuka et al. reported the development of a stable CHO cell line overexpressing the CHO ST6 (called ST6M).[46] They showed high sialylation level of the Fc portion of a human IgG1-based diabody, with ~44% of disialylated diantennary glycans (G2S2, G2FS2), and ~26% of G2FS1. Strikingly, while diabody Fc galactosylation in the parental cell line was relatively low (15% of digalactosylated G2F glycan), this level was highly enhanced in the ST6M cell line (76% of digalactosylated glycans overall; 6% as G2F and 70% as sialylated digalactosylated species). However, the mechanism leading to this highly enhanced galactosylation level in ST6M cell line was not discussed by the authors. Yet, similarly to in vitro mAb sialylation, the ST6M cell line generated a mAb with mostly disialylated glycans, which may not be physiologically relevant since G2FS1 is the main sialylated Fc glycan found in circulating human IgGs. In a paper published in 1999, Weikert et al. reported that the co-expression of human GT and ST3 with a TNFR-IgG1 Fc fusion protein resulted in >90% of the glycan branches terminated by a sialic acid.[45] However, the glycans considered in this estimation were the sialylated glycans only, i.e., the neutral glycans (G0F, G1F and G2F) were not taken into account. Moreover, no distinction was made between the glycans attached to the TNFR and the IgG Fc glycans. Thus, while the sialylation efficiency they obtained cannot be compared to our results despite the similarity of the methods, it is interesting to note that the co-expression of TNFR-Fc with GT resulted in an accumulation of G2F without sialylation improvement, as we observed for TZMGT and TZMmGT. Clark and coworkers also reported no sialylation improvement upon enhancement of the galactose content of an Fc-fusion protein following galactose feeding of a CHO cell culture.[49] They observed a concomitant increase of the intracellular sialidase content, and suggested that galactose up-regulated the production of sialidases in CHO cells, thus reducing sialylation. While the presence of intracellular sialidase activity participating in the generation of G2F glycan cannot be excluded, our data suggest other causes.

The IgG1 bearing the F243A substitution was produced to enlighten some of the restrictions encountered for the sialylation of the wild-type mAb. The phenylalanine 243 has been shown to be in contact with the GlcNAc residue of the α1,6-arm of the glycan.[10] The F243A substitution was shown to enhance galactosylation and sialylation levels of the Fc, presumably by allowing the glycan to span out of the cavity formed by the 2 Cγ2 domains of the IgG, thus increasing the glycan exposure to the galactosyl- and sialyltransferases.[9,33,40] More recently, Barb et al. proposed that the glycans were dynamic and alternating between 2 states, a state where the glycan is maintained within the cavity by the interactions of the α1,6-arm with the protein surface, and the other where both arms of the glycans are exposed outside of the Fc cavity and become accessible to glycosyltransferases.[50,51] Thus, the reduced glycan-protein interaction caused by the F243A substitution may destabilize the equilibrium between the 2 states in favor of the second.[50] As expected, TZMm expressed alone was highly galactosylated and sialylated, yet the expression of ST6 somewhat increased the sialylation level. However, the expression of GT resulted in increased galactosylation, but the sialylation level was lower than in TZMm and TZMmST6. In both TZMGT and TZMmGT, G2F was the major glycan observed. Thus, while our results support the conclusion that the F243-glycan interaction in the wild-type Fc impairs galactosylation and ST6-mediated sialylation of the glycans, it could not explain the lack of endogenous ST3-mediated sialylation of the galactosylated wild-type antibodies. The co-expression of GT

and ST6 in the F243A mutant resulted in >80% of sialylated glycans, and 76% of the complex branches terminated by a sialic acid. 85% of the sialic acids were α2,6-linked in TZMmGTST6, which is close to the 88% found in TZMGTST6. In contrast, only 63% of the sialic acids were of the α2,6-linkage type in TZMmST6, which is higher than the 47% observed by Jassal et al. using a F243A IgG3 co-expressed with the rat ST6.[33] Thus, our data suggest that the co-expression of both GT and ST6 in CHO cells favors α2,6 over α2,3 sialylation since the galactose residues provided by the overexpression of human GT are preferentially used by ST6 rather than ST3.

The close examination of the glycan isomers detected in our samples gives insights on the characteristics of transferases. First, the action of the endogenous GT and overexpressed human GT could not be distinguished. However, the galactose residue in G1F was present on the α1,6-arm of the glycan in all cases (endogenous CHO or human GT), suggesting they both have the same selectivity for this arm, a result in agreement with the reported selectivity found for the human GT.[52] Second, only one G2FS(6)1 isomer was detected. Given the branch selectivity of the human ST6[39,51], the sialic acid was considered to be on the galactose residue lying on the α1,3 arm. As for G1FS(6)1, only one isomer was detected, but we could not determine if the galactose and SA residues were on the α1,3- or α1,6-arm of the glycan.

The very low incidence of G1FS(6)1 could be explained by the opposed branch selectivity of GT and ST6: the α1,6-arm galactose being more abundant, but less favored by ST6, while the ST6s preferred α1,3-arm galactose residue being rare due to GT's selectivity. Interestingly, we found that G2FS2 is composed of G2FS(3,6)2 and G2FS(6,6)2 since G2FS(3,3)2 was never detected when ST6 was expressed. Thus, ST6 appears faster than ST3 to sialylate G2FS(3)1, which suggests that G2FS(3)1 carries the α2,3 sialic acid on the α1,6, leaving the free galactose residue on ST6s favorite α1,3 branch. This in turn indicates that CHO ST3 has the opposite arm selectivity to ST6, which had been suggested for the rat liver ST3 and ST6.[53] The hypothesis of ST3 selectivity for the α1,6-arm is supported by the relatively high amounts of G1FS(3)1 found in TZMm and TZMmST6.

Finally, it is reasonable to think that the α1,6-arm glycan's interaction with F243 residue hampers ST3 action as it also hampers CHO GT, human GT and ST6 by limiting glycan accessibility, a fortiori if ST3 is indeed selective for this α1,6-arm. The increased ST3-mediated sialylation of the mutant F243A Fc compared to the wild-type could be the simple consequence of the increase of galactose level due to the mutation, rather than the consequence of increased accessibility to the galactose. However, overexpression of the human GT did not enhance ST3-mediated sialylation as it rather reduced it with a concomitant accumulation of G2F glycan. Moreover, the G1FS(3)1 observed in TZMm and TZMmST6 dropped to trace levels when GT was expressed. This indicates that G2F may not be a very good substrate per se for the CHO endogenous ST3, which could actually strongly prefer the G1F glycan.

The successive reaction steps of the ST3 enzyme would thus be G1F→G1FS1→G2FS1 (through GT)→G2FS2, whereas the human ST6Gal1 would rather take the classic path G1F→G2F→G2FS1→G2FS2. Then, the rapid G1F to G2F conversion upon GT overexpression would consume ST3s preferred substrate. The studies on sialyltransferases' enzymatic activity usually consider G2F or Galβ1–4GlcNAc as substrates, and data comparing G1F isomers to G2F as acceptor substrates are missing.[54] Similarly, to our knowledge, G1FS1 has not been studied as acceptor substrate for the galactosyltransferases.[52,55-57] Thus, there is no data in the literature indicating that the presence of a sialic acid on one branch would be an obstacle for galactosylation of the other branch. A second hypothesis is that the absence of G2F α2,3-sialylation in TZMGT and TZMmGT could reflect the inability of ST3 to cooperate with the human GT, whereas human ST6 and human GT may form highly active complexes, as proposed by Hassinen and coworkers.[58]

In conclusion, we developed a method for the fast production of antibodies enriched in the glycan G2FS(6)1, which is the predominant sialylated glycan found in circulating human IgGs. This approach provides sufficient amounts of homogeneous material for structure-function and small animal studies. This work also provides valuable information to help delineate the contributions of the Fc structure, versus the inherent substrate particularities of the glycosyltransferases, that limit mAbs' sialylation in glyco-engineered CHO cells. Further understanding of these glycosylation processes would allow the design of cell lines producing mAbs with glycans tailored for therapeutic applications.

Materials and Methods

Cell line

CHO cells expressing a truncated Epstein-Barr virus Nuclear Antigen-1 (CHO-3E7) were grown in suspension in serum-free FreeStyle™ F17 medium (Invitrogen, cat# A13835–01) supplemented with 0.1% Kolliphor P188 (Sigma-Aldrich, cat# K4894) and 4 mM glutamine (Sigma-Aldrich, cat# G8540). Cultures were maintained between 0.1 and 2.0×10^6 cells/mL in 125 mL Erlenmeyer ventilated flasks shaken at 120 rpm in a humidified incubator at 37°C with 5% CO_2 (standard conditions). Cell density and viability were determined using the Cedex Innovatis automated cell counter Cedex Analyzer (Roche) based on the trypan blue exclusion method.

Plasmids

TZM is a humanized mouse IgG1 directed against the human epidermal growth factor receptor-2 (HER2 or Erb2). The wild-type and F243A mutant versions consist of a HC of the G1m17 allotype and a kappa LC of Km3 allotype. The non-glycosylated TZM mutant (N297Q) consists of the LC, coupled to a TZM HC variant of G1m17,1 allotype, with a truncated IgG3 hinge[59] and the N297Q substitution. The LC used has no N-glycosylation site, and HC and HCF243A contain only the N297 glycosylation site. The human GT and ST6 were expressed as the complete membrane-bound proteins. HC, HCF243A, HCN297Q, LC, ST6 and GT were each cloned in pTT5 vectors essentially as described previously.[60,61] The pTT vector encoding

the green fluorescent protein (GFP) was used as a reporter gene and has been described elsewhere.[62]

MAbs production

Linear deacylated polyethylenimine Max (PEImax) was obtained from Polysciences, (cat# 24765).[63] Stock solutions (3 mg/mL) were prepared in ultrapure water, sterilized by filtration (0.2 μm), aliquoted and stored at 4°C. Cells were diluted 1 day before transfection in fresh medium at 0.7×10^6 cells/mL. They were transfected with viability greater that 99% at densities between 1.5 and 2.0×10^6 cells/mL. DNA and PEImax mixes were separately prepared in complete F17 medium. DNA (1.5 μg/mL in the final culture volume) was added first to the suspension, which was incubated 5 min at 37°C before the addition of PEI (7 μg/mL final). 24 hours post-transfection (hpt), cells were fed with peptone TN1 (0.5% w/v final), and the culture temperature was shifted to 32°C. Transfection efficiency was assessed 24 hpt by determining the percentage of GFP positive cells by flow cytometry with a BD LSRII cytometer (BD Biosciences). Only viable single cells were taken into account.

Purification of mAbs from cell culture supernatants

Cell cultures were centrifuged 20 min at 3000 g 4 d post-transfection (dpt) at a viability > 60%. The supernatant was collected and loaded on a 4 mL MabSelect™ SuRe™ column (GE Healthcare, cat# 17–5438–02) equilibrated in PBS. The column was washed with PBS and mAbs were eluted with 100 mM citrate buffer pH 3.0. The fractions containing mAbs were pooled and the citrate buffer was exchanged against water on Econo-Pac→ 10DG columns (Bio-Rad, cat# 732–2010). Purified mAbs were sterilized by passing through 0.2 μm filters, aliquoted, and stored at −80°C.

Quantification of mAbs

MAbs titers in culture supernatants were determined by protein-A HPLC using a 800 μL POROS® 20 micron Protein A ID Cartridge (Applied Biosystems, cat# 2–1001–00) according to the manufacturer's recommendations. Purified mAbs were quantified by absorbance at 280 nm using a Nanodrop™ spectrophotometer (Thermo Fisher Scientific).

Sialidase digestions

α2,3-linked sialic acids were removed from the purified antibody (50–100 μg, 1–2 mg/mL), by the *Streptococcus pneumoniae* Glyko® Sialidase S™ (Prozyme, cat# GK80020) at 0.2 U/mL after 2 hours of incubation at 37°C in 250 mM phosphate buffer pH 6.0. All sialic acids (α2,3 and α2,6) were removed by incubation for 18 h at 37°C with the *Arthrobacter ureafaciens* Neuraminidase (MP Biomedicals, cat# 153846) at 0.05 U/mL in 250 mM phosphate buffer pH 5.0.

Lectin-blot

Biotinylated *Erythrina Cristagalli* agglutinin (ECL), *Sambucus Nigra* agglutinin (SNA) and *Maackia Amurensis* lectin II (MALII) (Vector Laboratories, cat# B-1145, B-1305 and B-1265, respectively) were used to evaluate terminal β1,4-galactosylation, α2,6-sialylation and α2,3-sialylation, respectively. The supernatants containing antibodies, as well as purified antibodies were treated with DTT (10 min at 70°C) to reduce disulfide bonds in order to visualize the mAb HCs separately from the LCs. 180 ng of mAbs were loaded for ECL and MALII-blots, while 120 ng were loaded for SNA-blots. After protein transfer, nitrocellulose membrane was incubated 2 hours with the lectin (3 μg/mL ECL, 1 μg/mL SNA or 10 μg/mL MALII), then one hour with 1:1000 Streptavidin-HRP (Sigma-Aldrich, cat# S2438). The membrane was thoroughly washed with PBS-Tween 0.05% before each incubation step. Ponceau red staining was used to control the amount of protein loaded. Signal was revealed with BM Chemiluminescence Blotting Substrate (POD) (Roche Applied Science, cat# 11500708001) and the images recorded with a Chemidoc MP Imaging System (Biorad).

cIEF

Charge profiles of the antibodies were obtained with the HT Protein Charge Variant kit on a LabChip® GX (Caliper Life Sciences). Purified mAbs at 1–2 mg/mL in water were prepared according to the manufacturer's recommendations. The conditions selected were 90 seconds assay length with the buffer pH 7.2. Desialylated mAbs were desalted on Illustra Microspin columns (GE Healthcare, cat# 27–5330–01) before analysis.

Glycoprofile analysis by LC-MS

Fc/2 (C_H2-C_H3) glycopeptides were obtained by digestion of the antibodies (20 μg, 2 mg/mL) with 20 U of "FabRICATOR" IdeS (Genovis) in 0.15 M NaCl, 0.05 M sodium phosphate, pH 6.6, at 37°C for 30 minutes. The resulting digests were analyzed by LC-MS using an Agilent HP1100 Capillary LC system (Agilent Technologies) coupled to a LTQ-Orbitrap XL mass spectrometer (Thermo Fisher Scientific) equipped with a high flow electrospray ionization source. One ug of digested antibody was loaded on a Poros R2 column (2.1 × 30 mm) (Applied Biosystems) heated to 80°C. Mobile phases were 0.1% formic acid in water (A) and 75% acetonitrile, 25% tetrahydrofuran (B) preheated to ∼80°C. A linear gradient of 10%-75% B over 12 minutes (1 mL/min) was used to resolve the Fc/2 and Fab antibody fragments. The HPLC eluent was split to 100 μL/min just before the electrospray source of the LTQ-Orbitrap XL and MS spectra was acquired from m/z 400 to 2000 at a resolution of 15,000. LC-MS spectra were viewed in Xcalibur® (Thermo Fisher Scientific). Molecular weight profiles were generated with the MassLynx© MaxEnt1 deconvolution software (Waters). Databridge (Waters) was used to convert the protein LC-MS spectra into a format that was compatible with MaxEnt1.

The abundances of the glycans were calculated on the basis of signal heights observed in the molecular weight profiles. The percentage of a given glycan was obtained as the signal height of the Fc/2 glycopeptide carrying this glycan divided by the total signal heights of the glycans identified in the profile. The glycans identified and taken into account in the total signal heights are presented in **Table 1**. In **Table 2**, the percentage of complex antennae terminated by a given monosaccharide residue or

containing a given monosaccharide residue represents the actual number of residues present on complex antennae divided by the total available positions for this residue in the complex glycans (for example, G0F contains 0 galactoses, but 2 available positions for galactose). Only the strictly complex glycans were taken into account, i.e., the hybrids G0F−GlcNAc and G1F−GlcNAc (see legend of **Table 2** for definitions) containing only one outer arm-GlcNAc residue, were not considered. For example, the percentage of complex antennae terminated by a galactose was calculated as follows:

% Gal-terminated complex antennae = 100 × (1 ×%G1F + 2 ×%G2F + 1 ×%G2FS1 + 3 ×%G3F) / (2 ×%G0F + 2 ×%G1F + 2 ×%G2F + 2 ×%G1FS1 + 2 ×%G2FS1 + 2 ×%G2FS2 + 3 ×%G3F + 3 ×%G3FS3).

Glycan analysis by HILIC

Glycan were released from the antibody using PNGase F (Promega, cat# V4831) at 37°C for 24 hours. The enzyme and the antibody were removed using prewashed 10K molecular weight cut-off filters, and the glycans were evaporated to dryness under vacuum. They were then labeled with 2-aminobenzamide (2-AB) (Sigma-Aldrich, cat# PP0520).[64] Glycans were analyzed by HILIC with fluorescent detection using a Waters X-Bridge 3.5 μm amide column (4.6 × 250 mm) with the column heated to 30°C and a flow rate of 0.86 mL/min. Glycans were eluted using 50 mM ammonium formate, pH 4.4 (mobile phase A) and acetonitrile (mobile phase B) starting with an initial ratio of 20:80, followed by a gradient to 50:50 over 48 minutes. Peaks were calibrated with a 2-AB labeled glucose ladder and glycan standards[65] (Prozyme, cat# GKSB-503) and compared to GU

values in Glycobase.NIBRT.ie. Structural assignment was also based on exoglycosidase analysis.[66] Broad specificity Glyko® sialidase A™ (Prozyme, cat# GK80040) and Sialidase S™ (Prozyme, cat# GK80020) were used for sialic acid digests according to the manufacturer's instructions.

The abundances of the glycans were calculated on the basis of peak areas observed in the chromatograms. The percentage of a given glycan was obtained as the peak area of the PNGaseF-released glycan divided by the sum of the areas of all the peaks detected in the chromatogram. The incidence of terminal α2,3 and α2,6SA residues was calculated among the sialylated di-antennae complex glycans only, i.e., G1FS(3)1, G1FS(6)1, G2FS(3)1, G2FS(6)1, G2FS(3,3)2, G2FS(3,6)2 and G2FS(6,6)2. For example, the percentage of sialylated complex antennae terminated by a α2,3SA was calculated using the following term:

% α2,3SA-terminated sialylated complex antennae = 100 × (1 ×%G1FS(3)1 + 1 ×%G2FS(3)1 + 2 ×%G2FS(3,3)2 + 1 ×%G2FS(3,6)2) / (1 ×%G1FS(3)1 + 1 ×%G1FS(6)1 + 1 ×%G2FS(3)1 + 1 ×%G2FS(6)1+ 2 ×%G2FS(3,3)2 + 2 ×%G2FS(3,6)2 + 2 ×%G2FS(6,6)2)

References

1. Chan AC, Carter PJ. Therapeutic antibodies for autoimmunity and inflammation. Nat Rev Immunol 2010; 10:301-16; PMID:20414204; http://dx.doi.org/10.1038/nri2761
2. Albanesi M, Daëron M. The interactions of therapeutic antibodies with Fc receptors. Immunol Lett 2012; 143:20-7; PMID:22553779; http://dx.doi.org/10.1016/j.imlet.2012.02.005
3. Scott AM, Allison JP, Wolchok JD. Monoclonal antibodies in cancer therapy. Cancer Immun 2012; 12:14; PMID:22896759
4. Arnold JN, Wormald MR, Sim RB, Rudd PM, Dwek RA. The impact of glycosylation on the biological function and structure of human immunoglobulins. Annu Rev Immunol 2007; 25:21-50; PMID:17029568; http://dx.doi.org/10.1146/annurev.immunol.25.022106.141702
5. Patel D, Guo X, Ng S, Melchior M, Balderes P, Burtrum D, Persaud K, Luna X, Ludwig DL, Kang X. IgG isotype, glycosylation, and EGFR expression determine the induction of antibody-dependent cellular cytotoxicity in vitro by cetuximab. CA Hum Antibodies 2010; 19:89-99.
6. Houde D, Peng Y, Berkowitz SA, Engen JR. Posttranslational modifications differentially affect IgG1 conformation and receptor binding. Mol Cell Proteomics 2010; 9:1716-28; http://dx.doi.org/10.1074/mcp.M900540-MCP200
7. Leatherbarrow RJ, Rademacher TW, Dwek RA, Woof JM, Clark A, Burton DR, Richardson N, Feinstein A. Effector functions of a monoclonal aglycosylated mouse IgG2a: binding and activation of complement component C1 and interaction with human monocyte Fc receptor. Mol Immunol 1985; 22:407-15; PMID:4033665; http://dx.doi.org/10.1016/0161-5890(85)90125-7
8. Tao MH, Morrison SL. Studies of aglycosylated chimeric mouse-human IgG. Role of carbohydrate in the structure and effector functions mediated by the human IgG constant region. J Immunol 1989; 143:2595-601; PMID:2507634
9. Wormald MR, Rudd PM, Harvey DJ, Chang S-C, Scragg IG, Dwek RA. Variations in oligosaccharide-protein interactions in immunoglobulin G determine the site-specific glycosylation profiles and modulate the dynamic motion of the Fc oligosaccharides. Biochemistry 1997; 36:1370-80; PMID:9063885; http://dx.doi.org/10.1021/bi9621472
10. Krapp S, Mimura Y, Jefferis R, Huber R, Sondermann P. Structural analysis of human IgG-Fc glycoforms reveals a correlation between glycosylation and structural integrity. J Mol Biol 2003; 325:979-89; PMID:12527303; http://dx.doi.org/10.1016/S0022-2836(02)01250-0
11. Voynov V, Chennamsetty N, Kayser V, Helk B, Forrer K, Zhang H, Fritsch C, Heine H, Trout BL. Dynamic fluctuations of protein-carbohydrate interactions promote protein aggregation. PloS One 2009; 4:e8425; PMID:20037630; http://dx.doi.org/10.1371/journal.pone.0008425
12. Holland M, Yagi H, Takahashi N, Kato K, Savage COS, Goodall DM, Jefferis R. Differential glycosylation of polyclonal IgG, IgG-Fc and IgG-Fab isolated from the sera of patients with ANCA-associated systemic vasculitis. Biochim Biophys Acta 2006; 1760:669-77; PMID:16413679; http://dx.doi.org/10.1016/j.bbagen.2005.11.021
13. Wuhrer M, Stam JC, van de Geijn FE, Koeleman CA, Verrips CT, Dolhain RJEM, Hokke CH, Deelder AM. Glycosylation profiling of immunoglobulin G (IgG) subclasses from human serum. Proteomics 2007; 7:4070-81; PMID:17994628; http://dx.doi.org/10.1002/pmic.200700289
14. Anumula KR. Quantitative glycan profiling of normal human plasma derived immunoglobulin and its fragments Fab and Fc. J Immunol Methods 2012; 382:167-76; PMID:22683540; http://dx.doi.org/10.1016/j.jim.2012.05.022
15. Ferrara C, Bru P, Suter T, Moser S, Pu U, Uman P. Modulation of therapeutic antibody effector functions by glycosylation engineering: influence of Golgi enzyme localization domain and co-expression of heterologous b1, 4-N-acetylglucosaminyltransferase III and Golgi a-mannosidase II. Biotechnol Appl Biochem 2006; 93:851-61.
16. Mizushima T, Yagi H, Takemoto E, Shibata-Koyama M, Isoda Y, Iida S, Masuda K, Satoh M, Kato K. Structural basis for improved efficacy of therapeutic antibodies on defucosylation of their Fc glycans. Genes Cells 2011; 16:1071-80; PMID:22023369; http://dx.doi.org/10.1111/j.1365-2443.2011.01552.x
17. Shields RL, Lai J, Keck R, O'Connell LY, Hong K, Meng YG, Weikert SH, Presta LG. Lack of fucose on human IgG1 N-linked oligosaccharide improves binding to human Fcgamma RIII and antibody-dependent cellular toxicity. J Biol Chem 2002; 277:26733-40; PMID:11986321; http://dx.doi.org/10.1074/jbc.M202069200

18. Shinkawa T, Nakamura K, Yamane N, Shoji-Hosaka E, Kanda Y, Sakurada M, Uchida K, Anazawa H, Satoh M, Yamasaki M, et al. The absence of fucose but not the presence of galactose or bisecting N-acetylglucosamine of human IgG1 complex-type oligosaccharides shows the critical role of enhancing antibody-dependent cellular cytotoxicity. J Biol Chem 2003; 278:3466-73; PMID:12427744; http://dx.doi.org/10.1074/jbc.M210665200

19. Hodoniczky J, Zheng YZ, James DC. Control of recombinant monoclonal antibody effector functions by Fc N-glycan remodeling in vitro. Biotechnol Prog 2005; 21:1644-52; PMID:16321047; http://dx.doi.org/10.1021/bp050228w

20. Nimmerjahn F, Anthony RM, Ravetch JV. Agalactosylated IgG antibodies depend on cellular Fc receptors for in vivo activity. Proc Natl Acad Sci USA 2007; 104:8433-7; PMID:17485663; http://dx.doi.org/10.1073/pnas.0702936104

21. Kaneko Y, Nimmerjahn F, Ravetch JV. Anti-inflammatory activity of immunoglobulin G resulting from Fc sialylation. Science 2006; 313:670-3; PMID:16888140; http://dx.doi.org/10.1126/science.1129594

22. Scallon BJ, Tam SH, McCarthy SG, Cai AN, Raju TS. Higher levels of sialylated Fc glycans in immunoglobulin G molecules can adversely impact functionality. Mol Immunol 2007; 44:1524-34; PMID:17045339; http://dx.doi.org/10.1016/j.molimm.2006.09.005

23. Anthony RM, Wermeling F, Karlsson MCI, Ravetch JV. Identification of a receptor required for the anti-inflammatory activity of IVIG. Proc Natl Acad Sci USA 2008; 105:19571-8; PMID:19036920; http://dx.doi.org/10.1073/pnas.0810163105

24. Guhr T, Bloem J, Derksen NIL, Wuhrer M, Koenderman AHL, Aalberse RC, Rispens T. Enrichment of sialylated IgG by lectin fractionation does not enhance the efficacy of immunoglobulin G in a murine model of immune thrombocytopenia. PloS One 2011; 6: e21246; PMID:21731683; http://dx.doi.org/10.1371/journal.pone.0021246

25. Leontyev D, Katsman Y, Ma X-Z, Miescher S, Käsermann F, Branch DR. Sialylation-independent mechanism involved in the amelioration of murine immune thrombocytopenia using intravenous gammaglobulin. Transfusion 2012; 52:1799–1805; PMID:22257295; http://dx.doi.org/10.1111/j.1537-2995.2011.03517

26. Käsermann F, Boerema DJ, Rüegsegger M, Hofmann A, Wymann S, Zuercher AW, Miescher S. Analysis and functional consequences of increased Fab-sialylation of intravenous immunoglobulin (IVIG) after lectin fractionation. PloS one 2012; 7:e37243; http://dx.doi.org/10.1371/journal.pone.0037243

27. Yu X, Vasiljevic S, Mitchell DA, Crispin M, Scanlan CN. Dissecting the molecular mechanism of IVIg therapy: the interaction between serum IgG and DC-SIGN is independent of antibody glycoform or Fc domain. J Mol Biol 2013; 425:1253-8; PMID:23416198; http://dx.doi.org/10.1016/j.jmb.2013.02.006

28. Yu X, Baruah K, Harvey DJ, Vasiljevic S, Alonzi DS, Song B-D, Higgins MK, Bowden Ta, Scanlan CN, Crispin M. Engineering hydrophobic protein-carbohydrate interactions to fine-tune monoclonal antibodies. J Am Chem Soc 2013; 135:9723-32; PMID:23745692; http://dx.doi.org/10.1021/ja4014375

29. Campbell IK, Miescher S, Branch DR, Mott PJ, Lazarus AH, Han D, Maraskovsky E, Zuercher AW, Neschadim A, Leontyev D, et al. Therapeutic effect of IVIG on inflammatory arthritis in mice is dependent on the Fc portion and independent of sialylation or basophils. J Immunol 2014; 192:5031-8; PMID:24760152; http://dx.doi.org/10.4049/jimmunol.1301611

30. Massoud AH, Yona M, Xue D, Chouiali F, Alturaihi H, Ablona A, Mourad W, Piccirillo CA, Mazer BD. Dendritic cell immunoreceptor: a novel receptor for intravenous immunoglobulin mediates induction of regulatory T cells. J Allergy Clin Immunol 2014; 133:853-63 e5; PMID:24210883; http://dx.doi.org/10.1016/j.jaci.2013.09.029

31. Harduin-Lepers A, Vallejo-Ruiz V, Krzewinski-Recchi MA, Samyn-Petit B, Julien S, Delannoy P. The human sialyltransferase family. Biochimie 2001; 83:727-37; PMID:11530204; http://dx.doi.org/10.1016/S0300-9084(01)01301-3

32. Dalziel M, McFarlane I, Axford JS. Lectin analysis of human immunoglobulin G N-glycan sialylation. Glycoconj J 1999; 16:801-7; PMID:11133020; http://dx.doi.org/10.1023/A:1007183915921

33. Jassal R, Jenkins N, Charlwood J, Camilleri P, Jefferis R, Lund J. Sialylation of human IgG-Fc carbohydrate by transfected rat alpha2,6-sialyltransferase. Biochem Biophys Res Commun 2001; 286:243-9; PMID:11500028; http://dx.doi.org/10.1006/bbrc.2001.5382

34. Zhao J, Simeone DM, Heidt D, Anderson MA, Lubman DM. Comparative serum glycoproteomics using lectin selected sialic acid glycoproteins with mass spectrometric analysis: application to pancreatic cancer serum. J Proteome Res 2006; 5:1792-802; PMID:16823988; http://dx.doi.org/10.1021/pr060034r

35. Anthony RM, Nimmerjahn F, Ashline DJ, Reinhold VN, James C, Ravetch JV. A recombinant IgG Fc that recapitulates the anti-inflammatory activity of IVIG. Science 2008; 320:373-6; PMID:18420934; http://dx.doi.org/10.1126/science.1154315

36. Oaks M, Taylor S, Shaffer J. Autoantibodies targeting tumor-associated antigens in metastatic cancer: sialylated IgGs as candidate anti-inflammatory antibodies. Oncoimmunology 2013; 2:e24841; PMID:23894724

37. Stadlmann J, Pabst M, Altmann F. Analytical and functional aspects of antibody sialylation. J Clin Immunol 2010; 30:S15-S9; http://dx.doi.org/10.1007/s10875-010-9409-2

38. Raju TS, Briggs JB, Chamow SM, Winkler ME, Jones AJ. Glycoengineering of therapeutic glycoproteins: in vitro galactosylation and sialylation of glycoproteins with terminal N-acetylglucosamine and galactose residues. Biochemistry 2001; 40:8868-76; PMID:11467948; http://dx.doi.org/10.1021/bi010475i

39. Barb AW, Brady EK, Prestegard JH. Branch-specific sialylation of IgG-Fc glycans by ST6Gal-I. Biochemistry 2009; 48:9705-7; PMID:19772356; http://dx.doi.org/10.1021/bi901430h

40. Lund J, Takahashi N, Pound JD, Goodall M, Jefferis R. Multiple interactions of IgG with its core oligosaccharide can modulate recognition by complement and human Fc gamma receptor I and influence the synthesis of its oligosaccharide chains. J Immunol 1996; 157:4963-9; PMID:8943402

41. Kaneko E, Niwa R. Optimizing therapeutic antibody function: progress with Fc domain engineering. BioDrugs 2011; 25:1-11; PMID:21033767; http://dx.doi.org/10.2165/11537830-000000000-00000

42. Rose RJ, van Berkel PHC, van den Bremer ETJ, Labrijn AF, Vink T, Schuurman J, Heck AJR, Parren PWHI. Mutation of Y407 in the CH3 domain dramatically alters glycosylation and structure of human IgG. mAbs 2013; 5:219-28; PMID:23406897; http://dx.doi.org/10.4161/mabs.23532

43. Lefranc M-P, Giudicelli V, Ginestoux C, Jabado-Michaloud J, Folch G, Bellahcene F, Wu Y, Gemrot E, Brochet X, Lane J, et al.. IMGT®, the international ImMunoGeneTics information system®. Nucleic Acids Res 2009; 37:D1006–D12; PMID:18978023; http://dx.doi.org/10.1093/nar/gkn838

44. Lee EU, Roth J, Paulson JC. Alteration of terminal glycosylation sequences on N-linked oligosaccharides of Chinese hamster ovary cells by expression of beta-galactoside alpha 2,6-sialyltransferase. J Biol Chem 1989; 264:13848-55; PMID:2668274

45. Weikert S, Papac D, Briggs J, Cowfer D, Tom S, Gawlitzek M, Lofgren J, Mehta S, Chisholm V, Modi N, et al. Engineering Chinese hamster ovary cells to maximize sialic acid content of recombinant glycoproteins. Nat Biotechnol 1999; 17:1116-21; PMID:10545921; http://dx.doi.org/10.1038/15104

46. Onitsuka M, Kim W-D, Ozaki H, Kawaguchi A, Honda K, Kajiura H, Fujiyama K, Asano R, Kumagai I, Ohtake H, et al. Enhancement of sialylation on humanized IgG-like bispecific antibody by overexpression of α2,6-sialyltransferase derived from Chinese hamster ovary cells. Appl Microbiol Biotechnol 2012; 94:69-80; PMID:22205442; http://dx.doi.org/10.1007/s00253-011-3814-1

47. Raymond C, Robotham A, Kelly J, Lattova E, Perreault H, Durocher Y. Production of highly sialylated monoclonal antibodies. In: Petrescu S, ed. Rijeka, Croatia: Intech; 2012.

48. Kumar N, Gammell P, Clynes M. Proliferation control strategies to improve productivity and survival during CHO based production culture: a summary of recent methods employed and the effects of proliferation control in product secreting CHO cell lines. Cytotechnology 2007; 53:33-46; PMID:19003188; http://dx.doi.org/10.1007/s10616-007-9047-6

49. Clark KJ-R, Griffiths J, Bailey KM, Harcum SW. Gene-expression profiles for five key glycosylation genes for galactose-fed CHO cells expressing recombinant IL-4/13 cytokine trap. Biotechnol Bioeng 2005; 90:568-77; PMID:15818560; http://dx.doi.org/10.1002/bit.20439

50. Barb AW, Prestegard JH. NMR analysis demonstrates immunoglobulin G N-glycans are accessible and dynamic. Nat Chem Biol 2011; 7:147-53; PMID:21258329; http://dx.doi.org/10.1038/nchembio.511

51. Barb AW, Meng L, Gao Z, Johnson RW, Moremen KW, Prestegard JH. NMR characterization of immunoglobulin G Fc glycan motion on enzymatic sialylation. Biochemistry 2012; 51:4618-26; PMID:22574931; http://dx.doi.org/10.1021/bi300319q

52. Ramasamy V, Ramakrishnan B, Boeggeman E, Ratner DM, Seeberger PH, Qasba PK. Oligosaccharide preferences of beta1,4-galactosyltransferase-I: crystal structures of Met340His mutant of human beta1,4-galactosyltransferase-I with a pentasaccharide and trisaccharides of the N-glycan moiety. CA J Mol Biol 2005; 353:53-67.

53. Weinstein J, de Souza-e-Silva U, Paulson JC. Sialylation of glycoprotein oligosaccharides N-linked to asparagine. J Biol Chem 1982; 257:13845-53; PMID:7142180

54. Hossler P, Goh LT, Lee MM, Hu WS. GlycoVis: visualizing glycan distribution in the protein N-glycosylation pathway in mammalian cells. Biotechnol Bioeng 2006; 95:946-60; PMID:16807922; http://dx.doi.org/10.1002/bit.21062

55. Blanken WM, van Vliet A, van den Eijnden DH. Branch specificity of bovine colostrum and calf thymus UDP-Gal: N-acetylglucosaminide beta-1,4-galactosyltransferase. J Biol Chem 1984; 259:15131-5; PMID:6439717

56. Paquet MR, Narasimhan S, Schachter H, Moscarello MA. Branch specificity of purified rat liver Golgi UDP-galactose: N-acetylglucosamine beta-1,4-galactosyltransferase. Preferential transfer of galactose on the GlcNAc beta-1,2-Man alpha-1,3-branch of a complex biantennary Asn-linked oligosaccharide. J Biol Chem 1984; 259:4716-21; PMID:6425277

57. Ramakrishnan B, Balaji PV, Qasba PK. Crystal structure of beta1,4-galactosyltransferase complex with UDP-Gal reveals an oligosaccharide acceptor binding site. J Mol Biol 2002; 318:491-502; PMID:12051854; http://dx.doi.org/10.1016/S0022-2836(02)00020-7

58. Hassinen A, Pujol FM, Kokkonen N, Pieters C, Kihlström M, Korhonen K, Kellokumpu S. Functional organization of Golgi N- and O-glycosylation pathways involves pH-dependent complex formation that is impaired in cancer cells. J Biol Chem 2011; 286:38329-40; PMID:21911486; http://dx.doi.org/10.1074/jbc.M111.277681

59. Redpath S, Michaelsen TE, Sandlie I, Clark MR. The influence of the hinge region length in binding of human IgG to human Fcgamma receptors. Hum Immunol 1998; 59:720-7; PMID:9796740; http://dx.doi.org/10.1016/S0198-8859(98)00075-5

60. Shi C, Shin YO, Hanson J, Cass B, Loewen MC, Durocher Y. Purification and characterization of a recombinant G-protein-coupled receptor, Saccharomyces cerevisiae Ste2p, transiently expressed in HEK293 EBNA1 cells. Biochemistry 2005; 44:15705-14; PMID:16313173; http://dx.doi.org/10.1021/bi051292p

61. Zhang J, Liu X, Bell A, To R, Nath T, Azizi A, Li J, Cass B, Durocher Y. Transient expression and purification of chimeric heavy chain antibodies. Protein Expression Purif 2009; 65:77-82; http://dx.doi.org/10.1016/j.pep.2008.10.011

62. Durocher Y, Perret S, Kamen A. High-level and high-throughput recombinant protein production by transient transfection of suspension-growing human 293-EBNA1 cells. Nucleic Acids Res 2002; 30:E9; PMID:11788735; http://dx.doi.org/10.1093/nar/30.2.e9

63. Use of PEI for transfection may be covered by existing intellectual property rights iUP, 013,240, European Patent 0,770,140, and foreign equivalents for which further information may be obtained by contacting licensing@polyplus-transfection.com

64. Bigge JC, Patel TP, Bruce JA, Goulding PN, Charles SM, Parekh RB. Nonselective and efficient fluorescent labeling of glycans using 2-amino benzamide and anthranilic acid. Anal Biochem 1995; 230:229-38; PMID:7503412; http://dx.doi.org/10.1006/abio.1995.1468

65. Guile GR, Rudd PM, Wing DR, Prime SB, Dwek RA. A rapid high-resolution high-performance liquid chromatographic method for separating glycan mixtures and analyzing oligosaccharide profiles. Anal Biochem 1996; 240:210-26; PMID:8811911; http://dx.doi.org/10.1006/abio.1996.0351

66. Royle L, Radcliffe CM, Dwek RA, Rudd PM. Detailed structural analysis of N-glycans released from glycoproteins in SDS-PAGE gel bands using HPLC combined with exoglycosidase array digestions. Methods Mol Biol 2006; 347:125-43; PMID:17072008